Cavitation-Mediated Fracture Energy

Dissipation in Polylactide at Rubbery Soybean

Oil-based Block Copolymer Interfaces Formed

via Reactive Extrusion

Baker W Kuehl, Austin Hohmann, Ting Han Lee, Michael Forrester, Nacu

Hernandez, Hannah Dietrich, Connor Smith, Sam Musselman, Grayson Tran, and

Eric W. Cochran*

Department of Chemical & Biological Engineering, Iowa State University, Ames, Iowa

50011, United States

E-mail: ecochran@iastate.edu

Abstract

Here we spearhead a new approach to biopolymer impact modification that demon-

strates superior performance whilst maintaining greater than 99% compostability. Us-

ing soybean-based monomers, a virtually untapped resource in terms of commercial

volume and overall cost, a series of hyper-branched block copolymers were synthesized

and melt processed with polylactide (PLA) to yield impact resistant all-polymer com-

posites. While PLA impact modification has been treated extensively, to date the

only practical solutions have relied on non-compostable petroleum-based rubbers. This

study illustrates the activity of energy-dissipation mechanisms like cavitation, classi-

cally relegated to well-entangled petroleum-based rubbers, in poorly entangled hyper-

branched soybean-based rubbers. Furthermore, we present a complete study of the

1

mechanical performance and morphology of these impact modified PLA composites. The significance of combining deformation theory with a scalable green alternative to petroleum based rubbers opens up a potential avenue for cheap compostable engineering thermoplastics.

Keywords

Biopolymers, soybean oil, poly(l-lactide), toughening, extrusion

Introduction

Poly(L-Lactide) (PLA) has been sought as a potential replacement for petroleum-based engineering thermoplastics like acrylonitrile-butadiene-styrene (ABS) and high impact polystyrene (HIPS). ABS and HIPS are durable materials with a wide range of applications; however, greenhouse emissions and accumulation of non-degradable plastics has made the continued use of these legacy materials less desirable. PLA, with its high strength and low cost is presently the only commercially relevant biopolymer with properties approaching those of ABS. Despite its promising mechanical strength and modulus, unmodified PLA suffers from low ductility and brittleness, mechanically akin to polystyrene (PS).

Plasticizers are one strategy to reduce brittleness. In PLA, plasticizers like % poly(ethylene glycol) increase ductility at the expense of modulus and strength. Property tuning through copolymerization has also been explored, such as with biobased caprolatone, ^{3–5} yielding PLA hybrids with tailored mechanical profiles. Unfortunately, prohibitive cost precludes low-value/high volume applications such as single-use plastics. Less-costly polymer blends also afford property optimization, although this is limited by sparing polymer-polymer miscibility. Compatibilizers that stabilize the interface between thermodynamically incompatible polymers can alleviate these limits, enabling a rich variety of heterogeneous polymer mixtures. HIPS and ABS adopt this strategy by polymerizing styrene or styrene-co-acrylonitrile

(SAN) in the presence of an initiator and rubbery polybutadiene (PB), which phase separates into a nanoscale rubber dispersion. PB domains arrest crack propagation through a cavitation-mediated stress dissipation mechanism that relieves triaxial tension in the matrix. ^{6,7} Stress is transformed from plane strain to plane stress, resulting in the formation of a large plastic zone. ⁸ Rubbery particles exhibit a critical volumetric strain required to induce cavitation, and the deformation phenomena increase monotonically with decreasing particle size. ^{9,10} Recently, Declet-Perez et al. presented SAXS patterns in block copolymer (BCP) reinforced epoxy under various states of deformation, finding a doubling of rubbery core volume beyond the yield point compared to undeformed specimens. Following cavitation, the voids continue to expand in response to increasing hydrostatic tension, promoting plastic deformation in the form of matrix shear yielding. This cavitation process allows for brittle thermoplastic matrices such as PS and SAN to retain their rigidity while improving impact resistance. ABS has shown tensile strength, elastic modulus, and impact strength values around 38 MPa, 1700 MPa, and 17.8 kJ/m², respectively. ¹¹

Many analogous strategies have been explored in PLA. For example, epoxy-modified polymers ¹² or amphiphlic BCPs ^{13,14} have been used to stabilize PLA-rubber interfaces. Wang et al showed that epoxidized polybutadiene (EPB) and epoxidized poly(styrene-b-epoxidized butadiene-b-styrene) (ESBS) with epoxy content up to 36 mol % and loadings as high as 30 wt % significantly increased the tensile toughness and impact strength. ^{15,16} Here, PLA is chain-extended with the EPBS domains through reactive extrusion, forming compatibilizing PLA-ESBS/PLA-EPB graft copolymers. SEM micrographs of the post-deformation IZOD bar fracture surfaces showed fibril formation and voids due to ESBS cavitation; in contrast, fracture surfaces of neat PLA are smooth. These ESBS-PLA blends exchanged a 23% reduction in tensile strength for an increase in elongation at break from 3.5% to 158.4%. Poly(ethylene oxide-block-polybutylene oxide) (PEO-BO) is another effective PLA toughener. ¹⁷ For low PEO molecular weights, PEO-BO BCPs were well-dispersed throughout the matrix as nanoscale spherical micelles. PLA-PB BCPs synthesized via anionic/ring

opening polymerization have also been prepared as high performance bulk materials with rubbery domains formed via microphase separation. ¹⁸ Core-shell rubber particles (CSPs) with PB or polybutyl acrylate cores are also effective at dosages > 20 wt% and can be dispersed through melt processing. ¹⁹ CSPs have a rigid polymer shell that integrates with the matrix through miscibility or reactivity. While these strategies have seen some success, the current state-of-the-art impact modifiers suffer from some combination of cost, high dosage requirements, and undesirable sustainability/end-of-life implications. Low-cost, bio-derived and bio-degradable alternatives have been elusive.

Vegetable oils, such as soybean oil, castor oil, and sunflower oil, are long chain fatty acid triglycerides that can be used as precursors to rubbery polymers. Soybean oil has unsaturation that can readily be functionalized. Epoxidized soybean oil (ESO) has been used extensively as a plasticizer or as a compatibilizer for polyesters. ²⁰ ESO's oxirane functionality reacts in situ with carboxylic acid groups during polyester extrusion, improving the interfacial adhesion between erstwhile immiscible blend components. Acrylated ESO (AESO) has been used for biobased thermosetting coatings. ²¹ Using reversible addition fragmentation chain transfer (RAFT) to suppress macrogelation, thermoplastic hyper-branched poly(AESO) (PAESO) and poly(acrylated epoxidized high oleic soybean oil) (PAEHOSO) can be prepared at a range of MW values. 22 The RAFT method can also be used to prepare soybean-based block copolymers like poly (styrene- $b\mbox{-AESO}$) (PS-PAESO). 23 PS-PAESO showed no entanglement plateau arising from its high degree of branching and intramolecular looping of the side chains. ²⁴ Hyperbranched polymers routinely show very large entanglement MW values, or even a complete absence of entanglements. For example, a hyperbranched poly(ethylene glycol) (PEG) showed entanglement MWs near 55 kDa compared with $\lessapprox 1$ kDa for linear PEG.²⁵

The absence of entanglements reduces elasticity and accordingly the energy *storage* capacity of the rubber. Such limitations may be expected to make these materials less ineffective as impact modifiers, and indeed many attempts using soybean oil-based materials have

shown only minor improvements in tensile toughness^{26–28} and negligible improvements in impact strength.²⁹ Moreover, the most successful impact modifier rubbers have been based on highly entangled and elastic PB, further reinforcing this notion. However, impact toughness has been shown to be mediated primarily through stress energy transfer through strong rubber/matrix interfaces leading to its *dissipation* through the irreversible cavitation process.

As such, we hypothesized that soy-based rubbers like PAESO could effectively dissipate fracture energy in brittle matrices like PLA if there were strong interfaces and a finely dispersed morphology. In this work, we report the development of soybean-based elastomers that improve both the tensile toughness and impact strength by 1–2 orders of magnitude in PLA matrices. This study explores three architectures that have varying effects on the resulting resin performance: PAESO (soybean-oil homopolymer, SHOP), poly(MAEHOSO-co-methyl methacrylate) statistical copolymers (SCOP), and poly(glycidyl methacrylate-block-AEHOSO) block copolymers (SBCP). Through the oxirane and acid functionalities in blends of these polymers with PLA, graft-copolymers form in-situ within the extruder barrel that stabilize the PLA/soybean interfaces to yield dispersions of rubbery micelles. SBCP blends formed oblate micelles that provided the highest level of toughening with minimal loss in modulus. The level of improvement is similar to petroleum based impact modifiers attributing to the cavitation phenomena. As little as 10 wt % of these bioderived hyper-branched polymer impact modifiers can be used to synthesize PLA composites that could pave the way to economically viable biodegradable toughened engineering thermoplastics.

Results and Discussion

The molecular characteristics of the SHOP, SCOP, and SBCP polymers along with the thermomechanical properties of their blends at 10 wt % with PLA are summarized in Table 1. The soybean-based monomers, (meth)acrylated epoxidized high oleic soybean oil (MAE-HOSO/AEHOSO), were prepared with 2.2 vinyl groups per molecule via ring opening es-

Table 1: Molecular characteristics of the polymers used in this study and thermomechanical properties of the 90:10 wt % IngeoTM 2500HP PLA:Modifier blends formed therefrom.

	Molecular Characteristics ^a			Blend Thermomechanical Properties ^b								
Sample Code ^c	Mn (kDa) ^e	W _{P(G)MMA}	$(\%)$ d $_{\mathbf{D}}$ $^{\mathbf{e}}$	σ (MPa)	E (GPa)	ε_b (%)	$U_T(MJ/m^3)$	$E_{Frac}(J/m)$	T_g (°C)	T_c (°C)	T_m (°C)	
PLA	112.0	-	1.88	67 ± 2	2.5 ± 0.1	3 ± 1	1 ± 1	76 ± 11	56 ± 1	100 ± 1	170 ± 1	
SHOP-A	500.0	-	-	43 ± 2	2.1 ± 0.2	59 ± 26	15 ± 7	132 ± 25	52 ± 1	109 ± 1	173 ± 1	
SHOP-B	500.0	-	-	46 ± 1	2.2 ± 0.2	83 ± 21	25 ± 6	80 ± 33	52 ± 1	103 ± 1	172 ± 1	
SCOP-A	500.0	25.3	-	40 ± 1	1.8 ± 0.2	101 ± 31	31 ± 9	145 ± 25	53 ± 1	111 ± 3	175 ± 1	
SCOP-B	500.0	42.4	-	40 ± 1	1.9 ± 0.3	68 ± 40	20 ± 11	49 ± 6	55 ± 1	111 ± 1	175 ± 1	
SCOP-C	500.0	61.0	-	60 ± 1	2.1 ± 0.2	10 ± 1	3 ± 1	21 ± 5	58 ± 1	115 ± 1	175 ± 1	
SBCP-A	20.0	10.9	4.74	65 ± 1	1.9 ± 0.1	82 ± 8	35 ± 5	181 ± 25	62 ± 1	108 ± 1	175 ± 1	
SBCP-B	33.6	16.2	2.56	66 ± 1	1.9 ± 0.2	112 ± 5	47 ± 1	228 ± 41	59 ± 1	104 ± 1	173 ± 1	
SBCP-C	44.5	15.7	3.83	62 ± 2	1.9 ± 0.1	93 ± 8	38 ± 2	77 ± 11	62 ± 1	107 ± 1	172 ± 1	
SBCP-D	74.5	13.3	2.81	65 ± 1	2.1 ± 0.1	44 ± 1	18 ± 1	90 ± 20	62 ± 1	100 ± 3	175 ± 1	

a: Molecular characteristics of the hyper-branched soybean polymer additive

terification with (meth)acrylic acid. A family of thermoplastic elastomers was subsequently produced using RAFT polymerisation to prevent the formation of thermosets prior to melt blending. An example of a RAFT scheme can be seen in (Figure S1). The soybean-based polymers were blended with PLA via reactive extrusion, targeting the carboxylic acid end groups of PLA and the oxirane moieties of the hyper-branched rubber. Kinetics of the reaction in-situ during melt processing is heavily dictated by substitution on the epoxide ring. The primary epoxy ring on poly(glycidyl methacrylate) (PGMA) is expected to be orders of magnitude more reactive than secondary epoxy rings on the AEHOSO backbone. This grants biobased rubbers a higher extent of reaction in shorter residence times; nonetheless, most epoxy rings are expected to react at highly elevated temperatures, stabilising the polymer-polymer interface.

SHOP-A is poly(methacrylated epoxidized high oleic soybean oil) (PMAEHOSO); SHOP-B is the analogous PAEHOSO homopolymer. Statistical copolymers (SCOP) of PMMA and PMAEHOSO ranging from ca. 25 to 60 wt % PMMA were also prepared. The nominal number average molecular weight of these hyperbranched rubbery polymers is $M_n \approx 500$ kDa per

b: Thermomechanical properties of Ingeo 2500HP PLA Blends w/ 10wt% polymer additive

c:PLA = poly(L-lactide); SHOP = poly(meth)acrylated epoxidized high oleic soybean oil homopolymer; SCOP = polymethyl methacrylate-stat-polymethacrylated epoxidized high oleic soybean oil; SBCP = polyglycidyl methacrylate-block-poly acryalted epoxidized high oleic soybean oil

d:Weight fraction of either PMMA or PGMA was calculated based on HNMR results.

e: Dispersity and Mn for PLA was determined using gel permeation chromatography with THF as the mobile phase calibrated with PMMA standards. For SCOP and SHOP polymers, Mn was approximated using the target molecular weight for the polymerization as the polymer was too large to undergo filtration prior to GPC.

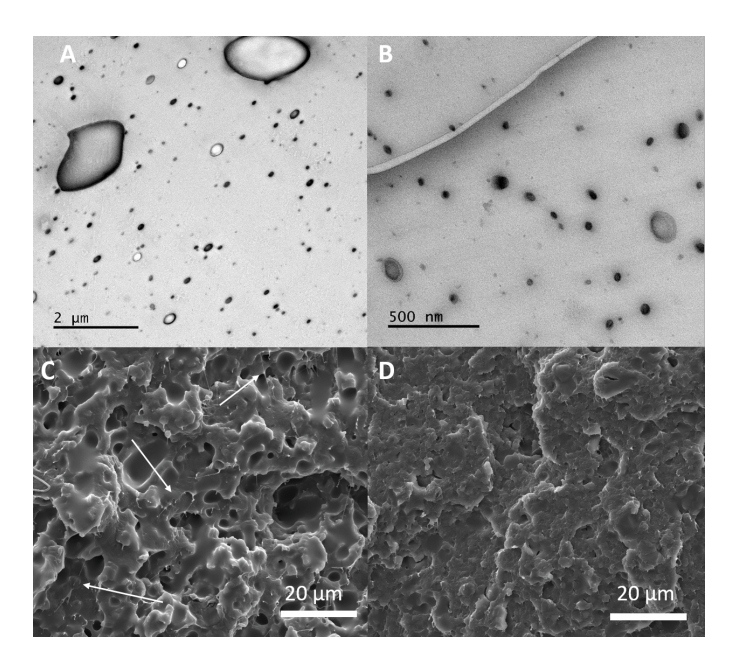


Figure 1: TEM and SEM micrographs of SHOP-A and SHOP-B. A) SHOP-A cryofractured tensile bar with preserved morphology. B) SHOP-B of the preserved morphology. C) Fracture surface of the SHOP-A IZOD specimen. D) Fracture surface of the SHOP-B IZOD specimen. The white arrows indicate the presence of a small amount of fibrils in the polymer composite.

the ratio of their mass to the number of moles of RAFT chain transfer agent. SHOP/SCOP GPC was not available because solutions of these polymers could not be passed through a filter, likely indicating the presence of microgels in spite of their melt processibility. The block copolymers (SBCP) were synthesized sequentially with glycidyl methacrylate followed by AEHOSO to form poly(glycidyl methacrylate-b-acrylated epoxidized high oleic soybean oil) (PGMA-PAEHOSO). The SBCP series feature roughly fixed PGMA composition (≈ 15 wt %) and $M_n \in 20$ –75 kDa. The hyperbranched soy-based "rubbers" are non-entangled as evidenced by the nonappearance of a plateau modulus in the dynamic shear rheology (Figure S2). In these materials, side-chains dominate the viscoelastic response, stiffening and diluting the relaxation of the primary chain. DSC and GPC traces can be found in the ESI (Figures S3 and S4).

(Figure S5) illustrates the various soybean-based polymer architectures. Homopolymers, statistical copolymers, and block copolymers have all been reported to toughen thermo-

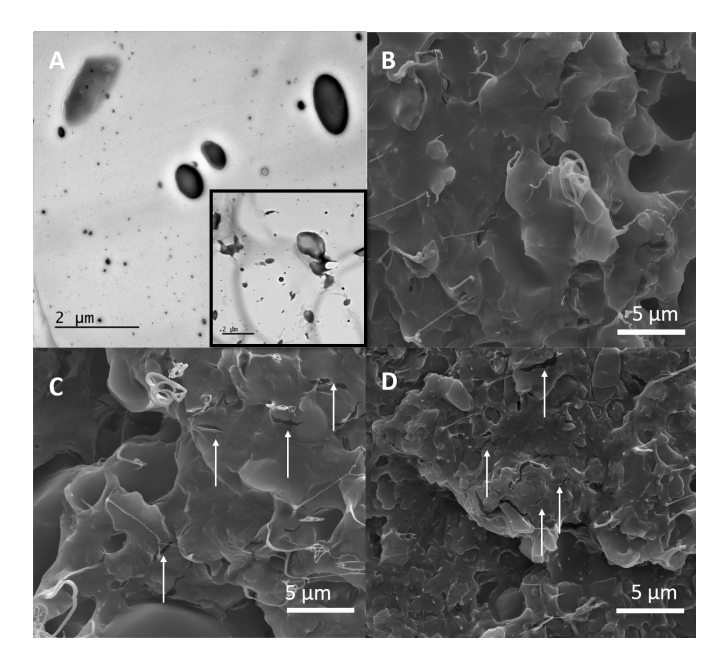


Figure 2: TEM and SEM micrographs of SCOP-A, SCOP-B, and SCOP-C. A) TEM micrograph of SCOP-A cryofractured tensile bar with preserved morphology. The inset in A) is a TEM micrograph of SCOP-A of the whitened gauge region of the tensile bar post deformation. B) SEM micrograph of SCOP-A fractured IZOD surface. C) SEM micrograph of SCOP-B fractured IZOD surface. D) SEM micrograph of SCOP-C fractured IZOD surface. The white arrows indicate surface cracks on IZOD specimen

plastics to varying degrees. ^{31,32} While there is information consistent with soybean based monomers being able to improve the tensile toughness of PLA blends with the use of compatibilizers, there is a lack of information of soybean based polymeric impact modifiers. We suspected with polymeric soybean modifiers the performance would be dramatically improved. Traditional soybean monomers, absent of crosslinking, are primarily known as plasticizers; however, the quality of plasticization will be poor. One issue with monomeric soybean impact modifiers is immiscibility with the PLA matrix, resulting in macroscopic features and poor mechanical properties. ²⁹ We found that in the SHOP blend, PAEHOSO was well distributed throughout the PLA matrix as shown in Figure 1A. We hypothesize that PAEHOSO residual epoxy rings formed graft-copolymers in-situ with PLA during melt processing, reducing the PLA/PAEHOSO interfacial energy. The excessive amount of ester linkages could also be a factor in improving the interfacial adhesion. ³³

Izod impact and tensile data for SHOP blends appear in Table 1. Figure 1A,B shows

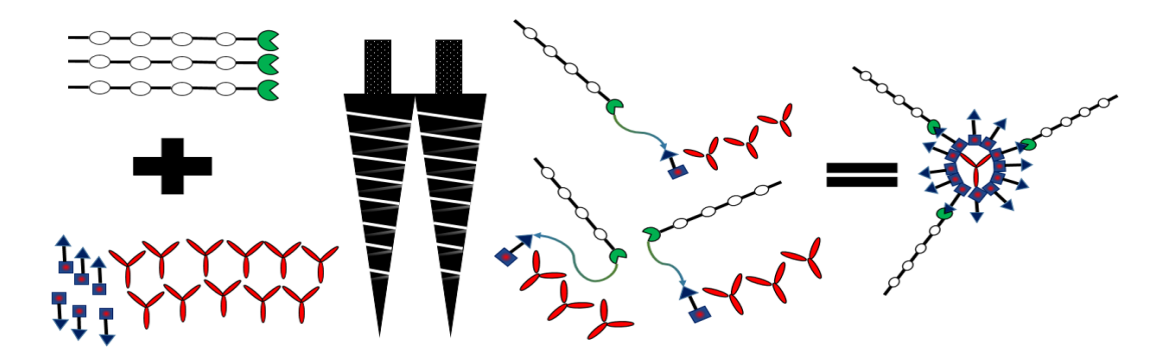


Figure 3: Cartoon depiction of the self-assembly process that occurs within the extruder barrel. The Male-Female connectors demonstrates the reactive extrusion process in-situ forming covalent bonds between the PGMA male connectors and the PLA Female connectors

TEM micrographs of the SHOP-A and SHOP-B blend morphology, respectively. SHOP-A phase separates into micelles ≈ 20 nm in diameter with a significant population of larger $\approx 2\mu \text{m}$ domains. SHOP-B, on the other hand, forms micelles in the 40–100nm range with no observable macrodomains. SHOP-A and SHOP-B differ by their acrylic backbones; SHOP-A has a methacrylic backbone and SHOP-B has an acrylic backbone. PLA is miscible with PMMA due to a negative Flory-Huggins interaction parameter.³⁴ Based on this, we speculated that there would be better compatibility in the PLA/PMAEHOSO (SHOP-A) pair compared to SHOP-B. This would be manifested by both a smaller domain size and stronger interfacial adhesion. SHOP-A does indeed show smaller micelles than SHOP-B, with the notable exception of the larger $2\mu m$ macrodomains. These latter features may be understood through the melt viscosity of SHOP-A vs. SHOP-B as shown in (Figure S6). Given the three order-of-magnitude viscosity difference over SHOP-B, evidently more compounding time and shear energy would be required to fully disperse the SHOP-A blend. Nonetheless, the superior interfacial adhesion of SHOP-A is manifested through its superior tensile and impact strength properties. While the acrylic SHOP-B presented a slightly higher elongation at break (83%) compared to (59%) in methacrylic SHOP-A, the latter exhibits an large improvement in impact strength (132 J/m) while the acrylic backbone exhibited negligible enhancement. SEM micrographs of the IZOD fracture surfaces (Figure 1D) reveal fairly smooth surface; this is indicative of poor plastic deformation under high frequencies.³⁵ Conversely, the methacrylic SHOP-A does undergo plastic deformation during impact testing as evidenced by Figure 1C. The images shows evidence of fibril extrusion from the surface, parallel to the direction of deformation, which dissipates mechanical energy leading to increased impact strength.³⁶

Noting the improved performance of the methacrylic backbone SHOP-A, evidently owing to its superior interfacial adhesion, we posited that further improvements could be achieved by further increasing the compatibility by introducing MMA counits in the SCOP series. Figure 2A shows the morphology of the SCOP-A blend. Surprisingly, the introduction of PMMA into the backbone led to a coarser dispersion of fairly spherical domains 100s of nm in extent. This suggests that dynamic vs. thermodynamic factors dominate the morphology, attributable to the higher melt viscosity of SCOP vs. SHOP as shown in (Figure S6). Surprisingly, SCOP-A is 2 orders of magnitude more viscous compared to PAEHOSO. The significantly higher melt viscosity leads to poor dispersion in the extruder resulting in larger features. A significantly higher viscosity could be the result of the primary chain being considerably larger than the PAEHOSO counterpart resulting from the steric hindrance of the methyl groups causing less intramolecular looping. The SCOP series also presents itself with viscosity values similar to PMAEHOSO; however, SCOP-A demonstrates a slightly lower viscosity. Nonetheless, all polymers show 2-3 order of magnitude increase from PAEHOSO. Longer residence times or more intense shear fields are required to produce a finer rubber phase dispersion. However, smaller features are not necessarily ideal for the purpose of impact toughening. When the rubber inclusions become too small, they fail to dissipate mechanical energy since they become essentially homogenized with the matrix. ³⁷ The inset in Figure 2A presents the SCOP-A morphology post deformation. The copolymer droplets undergo a transformation from roughly spherical particles to a wide variety of heterogeneous shapes. Upon incorporation of deformation into the PLA matrix, the droplets are being pulled in the direction parallel to the direction of an applied stress which improves the mechanical performance from elongation at break values of (59%) to (101%). Increasing the MMA composition in SCOP-B,C yielded embrittled materials due to excessive glassy content with T_g values of -4 and 48 °C) , respectively. Interestingly, SCOP-B contains 2 glass transition temperatures corresponding to MMA-rich and PMAEHOSO-rich domains, indicating partial phase separation shown in (Figure S7). Figures 2B, 2C, and 2D show SEM micrographs of the IZOD fracture surfaces of each copolymer blend. SCOP-A displays presence of large extended fibrils without the presence of surface cracks. SCOP-B and SCOP-C have large surface cracks (white arrows in Figure 2) indicating upon high rates of deformation, the PLA blend cannot dissipate mechanical energy. The crack formation could be from decreased phase separation of the soybean elastomer due to the strong interfacial adhesion. The SCOP series demonstrated that PMAEHOSO copolymers were most effective at impact modification with larger feature size and stronger adhesion to the PLA matrix. However, the loss of rubbery character as too many MMA segments are introduced suggested the need for an alternate strategy to meet these design goals.

The SBCP series features PGMA-b-PAEHOSO block copolymers at fixed PGMA composition over a range of MW values. These were hypothesized to efficiently form strong bonds with the matrix through the highly reactive primary epoxy pendant groups and PLA miscible of the PGMA block. The low-Tg rubbery PAEHOSO block has poor matrix solubility, and can strongly microphase separate without loss of interfacial adhesion or softening of the PLA phase. The design philosophy of the SBCP blends are illustrated in the cartoon of Figure 3. In this schematic, male and female connectors represent PGMA oxiranes and PLA acid groups, respectively that efficiently merge in the reactive extrusion process to form PAEHOSO cores stabilized by covalently attached PGMA-graft-PLA coronae. 32

The SBCP series impact strength was strongly MW dependent; some mechanistic insight to this can be inferred by comparison of the fracture surface morphology as seen in (Figure S8). (Figures S8 A,E) and (Figures S8 B,F) demonstrate extreme differences in topography for the lower MW SBCP-A and SBCP-B specimen as compared to higher-MW SBCP-C and

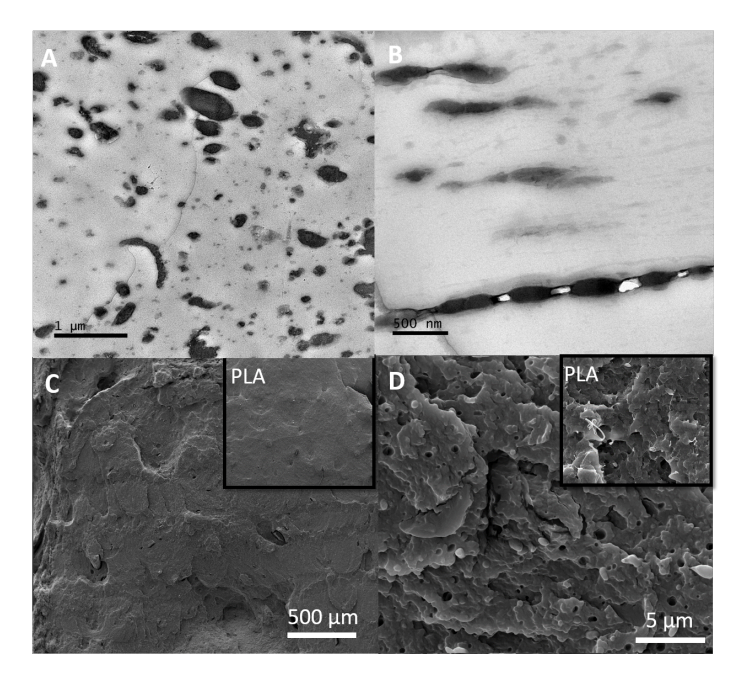


Figure 4: A) TEM micrograph of SBCP-A showing a mixture of wormlike micelles and vesicles distributed throughout the PLA matrix. B) TEM micrograph of SBCP-A post deformation showing internal cavitation throughout the PGMA-b-PAEHOSO micelle inhibiting crack propagation. C) SEM micrograph of SBCP-A showing the surface of the IZOD specimen post deformation. The inset in C is the surface of PLA post deformation. D) A high MAG SEM micrograph of the surface of the SBCP-A IZOD specimen further showing cavitated rubber particles. The onset in D shows the high MAG SEM micrograph of PLA.

SBCP-D (Figures S8 C,G and Figures S8 D,H); respectively. This can be attributed to an ability to dissipate the crack propagation. At higher magnification, (Figures S8 E,F) reveal large voids next to propagating cracks. The crack propagation is dissipated due to formation of large micron sized voids from the soybean elastomer. Figures (Figures G,H) show surface cracks that are not accompanied by elastomeric void formation, explaining the negligible increases in impact strength. A distinct difference can be seen as to why the SBCP blends display superior toughening effects over the other PAEHOSO elastomer counterparts. The observed void formation parallels the cavitation-mediated deformation mechanisms seen in high impact polystyrene. Shang et al. observed similar mechanical property performance with polybutylene terephalate (PBT) toughened with polyoctene ethylene (POE) compatibilized by POE-g-PGMA. Shang An increase in loading of POE-g-PGMA resulted in a decrease in both the impact strength and the elongation of the polymer composite. Since PGMA reacts

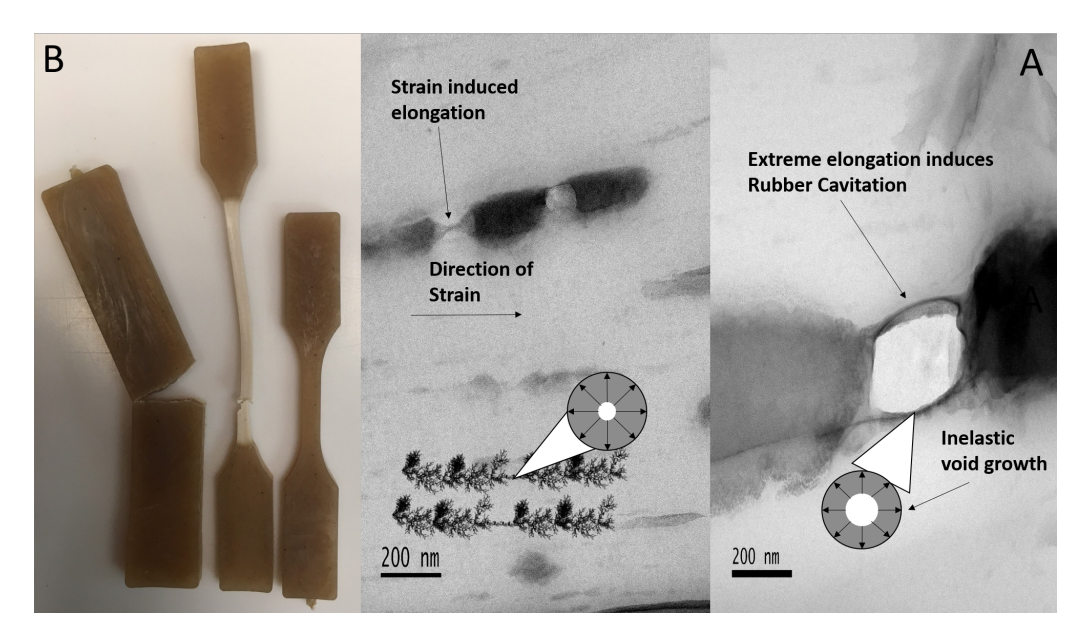


Figure 5: A) TEM micrograph of the cavitation behavior resulting from the strain induced elongation of the vitreous polymer micelles. B) An image of tensile bars pre- and post-deformation along with an IZOD bar post deformation

with polyesters, an increase in the epoxide content can yield smaller particle sizes or lead to possible crosslinking of the matrix resulting in the absence of rapid matrix shear yielding. This is analogous to the SBCP series as an increase in molecular weight of the PGMA block results in a superficial increase in epoxy loading. Due to the amount of carboxylic acids remaining constant, an increase in epoxy content can yield interactions similar to those seen in reactive blends of PBT.

The structure property difference between each soybean architecture can be viewed in Figure 4B where a drastic difference from the shape of the dispersed soybean elastomers can be seen. PGMA-b-PAEHOSO organizes into rod-like micelles while the other architectures seem to organize into roughly spherical micelles. The heterogeneous micelles results from the relatively low molecular weight of the block copolymer. Liu et al. polymerized similar molecular weight amphiphilic poly(ethylene-alt-propylene)-b-poly(ethylene oxide) which also resulted in more pronounced worm-like micelles. After deformation, the morphology can be seen in Figure 4B. TEM further supports the SEM images previously indicating rubber cavitation in the soybean based elastomer. Formation of these voids is due to a stable

interface created by having PGMA being both matrix miscible and reactive with the PLA matrix. The PGMA block will favor the PLA interface due to enthalpic interactions while the PAEHOSO block will segregate towards the center of a micelle forming the unique coreshell micelle structure. While statistical copolymers and homopolymers present a dispersed rubber, a lack of the unique core-shell micelle structure presents a deficiency in an ability to undergo cavitation. A lack of a cavitation mechanism directly affects the IZOD performance since the elastomer must be able to dissipate large amounts of energy in short time periods. While the homopolymer and statistical copolymers exhibit exemplary tensile performance, likely due to the ability to undergo shear yielding, the lack of cavitation presents a problem when dissipating energy quickly. Figure 4C displays the IZOD surface after impact of SBCP-A with the onset showing PLA. The PLA surface exhibits an extremely flat and pristing surface indicating a quick brittle failure under high frequency deformation; however, SBCP-A shows a high amount of surface roughness indicating a significant amount of plastic deformation. Upon observation of the impact surfaces under high magnification shown in Figure 4D, SBCP-A demonstrates a well dispersed PGMA-PAEHOSO rubber with micron sized voids further indicating the PGMA-PAEHOSO undergoes a cavitation mechanism for energy dissipation. The mechanism for onset of cavitation can be seen in Figure 5A The PGMA-PAEHOSO rod-like micelle is elongated in the direction parallel to the direction of strain. As a micelle reaches a critical strain, rather than the polymer tearing, a microscopic void forms which continues to grow to a macroscopic hole. As the macroscopic void reaches a critical size, the void is propagated through the micelle further dissipating more energy. The void formation leads to necking behavior and hinged breaks shown in Figure 5B. A composition study of the highest performing blend, SBCP-B, was performed on tensile testing shown in (Figure S9). At 2 wt % modifier loading, no improvement can be seen, likely due to the lack of phase separation from a high interfacial adhesion between the PLA matrix and the dispersed phase. However, upon the addition of 5 wt% modifier, a clear increase in the tensile elongation can be seen from 3% to 60%. Along with Instron tensile testing, IZOD

testing with SBCP-B blends at varying loadings was also performed. (Figure S10) contains small improvements in impact strength with the addition of 2 and 5 wt %; however, after the addition of 8 wt %, a doubling in the impact strength can be observed with a maximal impact strength achieved at our highest loading that was tested.

Conclusion

Our results challenge the notion that highly entangled rubbers are required for toughening of thermoplastic matrices. A family of soybean based rubbers were synthesized via RAFT polymerization and thoroughly dispersed throughout the PLA matrix using reactive extrusion. Tailoring the interfacial adhesion with diverse polymer architectures allowed for the formation of 200–500 nm soybean rubbers. With the absence of a highly entangled rubber, the bio-derived polymers effectively toughened the PLA matrix with < 10 wt% rubber loading. From the results, we deduced that reactive block copolymers could maximize the mechanical properties of PLA arising from rubber particle cavitation. The discovery of hyper-branched polymers significantly improving the ductility of thermoplastic matrices provides exciting new opportunities for the further valorization of other biobased polymers. The approach demonstrated here is both economical and commercially scalable allowing for the displacement of conventional petroleum derived impact modifiers.

Conflicts of Interest

There are no conflicts of interest to declare.

Supporting Information Available

The Supporting Information is available free of charge. Experimental details are listed including the synthetic scheme, plots of viscoelastic properties of the polymers, additional

SEM micrographs, DSC plots, GPC analysis, and extra mechanical testing data.

Acknowledgement

This work was funded by Center for Bioplastics and Biobased Composites. The authors acknowledge the assistance of Tracey Pepper Stewart and Warren Straszheim in their knowledge and expertise in electron microscopy.

References

- (1) Hottle, T. A.; Bilec, M. M.; Brown, N. R.; Landis, A. E. Toward zero waste: Composting and Recycling for Sustainable Venue Based Events. Waste Management 2015, 38, 86–94, DOI: 10.1016/j.wasman.2015.01.019.
- (2) Jacobsen, S.; Fritz, H. G. Plasticizing Polylactide—the Effect of Different Plasticizers on the Mechanical Properties. <u>Polymer Engineering & Science</u> 1999, 39, 1303–1310, DOI: https://doi.org/10.1002/pen.11517, _eprint: https://onlinelibrary.wiley.com/doi/pdf/10.1002/pen.11517.
- D. W.; J. (Co)polymers (3) Grijpma, Pennings, Α. of L-lactide, Me-1994, chanical Properties. Macromolecular Chemistry Physics and 195, 1649 - 1663, DOI: 10.1002/macp.1994.021950516, _eprint: https://onlinelibrary.wiley.com/doi/pdf/10.1002/macp.1994.021950516.
- (4) Jing, F.; Hillmyer, M. A. A Bifunctional Monomer Derived from Lactide for Toughening Polylactide. <u>Journal of the American Chemical Society</u> 2008, <u>130</u>, 13826–13827, DOI: 10.1021/ja804357u.
- (5) Hiljanen-Vainio, M.; Karjalainen, T.; Seppälä, J. Biodegradable Lactone Copolymers. I. Characterization and Mechanical Behavior of Caprolactone and Lac-

- tide Copolymers. <u>Journal of Applied Polymer Science</u> **1996**, <u>59</u>, 1281–1288, DOI: 10.1002/(SICI)1097-4628(19960222)59:8<1281::AID-APP11>3.0.CO;2-9, _eprint: https://onlinelibrary.wiley.com/doi/pdf/10.1002/%28SICI%291097-4628%2819960222%2959%3A8%3C1281%3A%3AAID-APP11%3E3.0.CO%3B2-9.
- (6) Yang, J.; Liu, J. Cavitation of Rubber Particles in High-Impact Polystyrene. <u>Polymer Journal</u> **2001**, <u>33</u>, 952–954, DOI: 10.1295/polymj.33.952, Number: 12 Publisher: Nature Publishing Group.
- (7) Wang, F.; Chang, L.; Hu, Y.; Wu, G.; Liu, H. Synthesis and Properties of In-Situ Bulk High Impact Polystyrene Toughened by High Cis-1,4 Polybutadiene. <u>Polymers</u> 2019, <u>11</u>, 791, DOI: 10.3390/polym11050791.
- (8) Bagheri, R.; Pearson, R. A. Role of Particle Cavitation in Rubber-Toughened Epoxies: 1. Microvoid Toughening. <u>Polymer</u> 1996, <u>37</u>, 4529–4538, DOI: 10.1016/0032-3861(96)00295-9.
- (9) Declet-Perez, C.; Francis, L. F.; Bates, F. S. Cavitation in Block Copolymer Modified Epoxy Revealed by In Situ Small-Angle X-Ray Scattering. <u>ACS Macro Letters</u> 2013, 2, 939–943, DOI: 10.1021/mz4004419.
- (10) Long, T. R.; Elder, R. M.; Bain, E. D.; Masser, K. A.; Sirk, T. W.; Yu, J. H.; Knorr, D. B.; Lenhart, J. L. Influence of Molecular Weight between Crosslinks on the Mechanical Properties of Polymers Formed via Ring-Opening Metathesis. <u>Soft Matter</u> 2018, 14, 3344–3360, DOI: 10.1039/C7SM02407J.
- (11) Hirayama, D.; Saron, C. Morphologic and Mechanical Properties of Blends from Recycled Acrylonitrile-Butadiene-Styrene and High-Impact Polystyrene. <u>Polymer</u> **2018**, 135, 271–278, DOI: 10.1016/j.polymer.2017.12.038.
- (12) Liu, H.; Chen, F.; Liu, B.; Estep, G.; Zhang, J. Super Toughened Poly(lactic acid)

- Ternary Blends by Simultaneous Dynamic Vulcanization and Interfacial Compatibilization. Macromolecules **2010**, 43, 6058–6066, DOI: 10.1021/ma101108g.
- (13) Gu, L.; Nessim, E. E.; Li, T.; Macosko, C. W. Toughening Poly(lactic acid) with Poly(Ethylene Oxide)-Poly (Propylene Oxide)-Poly (Ethylene Oxide) Triblock Copolymers. Polymer **2018**, 156, 261–269.
- (14) Xu, Y.; Thurber, C. M.; Macosko, C. W.; Lodge, T. P.; Hillmyer, M. A. Poly(methyl methacrylate)-block-polyethylene-block-poly(methyl methacrylate) Triblock Copolymers as Compatibilizers for Polyethylene/Poly(methyl methacrylate) Blends. <u>Industrial & Engineering Chemistry Research</u> 2014, <u>53</u>, 4718–4725, DOI: 10.1021/ie4043196, Publisher: American Chemical Society.
- (15) Wang, Y.; Wei, Z.; Leng, X.; Shen, K.; Li, Y. Highly Toughened Polylactide with Epoxidized Polybutadiene by In-Situ Reactive Compatibilization. <u>Polymer</u> **2016**, <u>92</u>, 74–83, DOI: 10.1016/j.polymer.2016.03.081.
- (16) Wang, Y.; Wei, Z.; Li, Y. Highly Toughened Polylactide/Epoxidized Poly(Styrene-b-Butadiene-b-Styrene) Blends with Excellent Tensile Performance. <u>European Polymer Journal</u> **2016**, 85, 92–104, DOI: 10.1016/j.eurpolymj.2016.10.019.
- (17) Li, T.; Zhang, J.; Schneiderman, D. K.; Francis, L. F.; Bates, F. S. Toughening Glassy Poly(lactide) with Block Copolymer Micelles. <u>ACS Macro Letters</u> **2016**, <u>5</u>, 359–364, DOI: 10.1021/acsmacrolett.6b00063.
- (18) Lee, I.; Panthani, T. R.; Bates, F. S. Sustainable Poly(lactide-b-butadiene) Multiblock Copolymers with Enhanced Mechanical Properties. <u>Macromolecules</u> 2013, <u>46</u>, 7387–7398, DOI: 10.1021/ma401508b, Publisher: American Chemical Society.
- (19) Fu, N.; Li, G.; Zhang, Q.; Wang, N.; Qu, X. Preparation of a Functionalized Core–Shell Structured Polymer by Seeded Emulsion Polymerization and Investigation

- on Toughening Poly(Butylene Terephthalate). RSC Adv. **2014**, $\underline{4}$, 1067–1073, DOI: 10.1039/C3RA44163F.
- (20) Han, Y.; Shi, J.; Mao, L.; Wang, Z.; Zhang, L. Improvement of Compatibility and Mechanical Performances of PLA/PBAT Composites with Epoxidized Soybean Oil as Compatibilizer. <u>Industrial & Engineering Chemistry Research</u> 2020, <u>59</u>, 21779–21790, DOI: 10.1021/acs.iecr.0c04285.
- (21) Tang, Q.; Li, Q.; Luo, Y.; Pan, X.; Xi, Z.; Zhao, L. Development of an Innovative Biobased UV Coating Synthesized from Acrylated Epoxidized Soybean Oil and Poly(Octamethylene Maleate (Anhydride) Citrate). <u>Industrial & Engineering</u> Chemistry Research **2021**, 60, 9797–9806, DOI: 10.1021/acs.iecr.1c01258.
- (22) Lin, F.-Y.; Yan, M.; Cochran, E. W. Gelation Suppression in RAFT Polymerization.

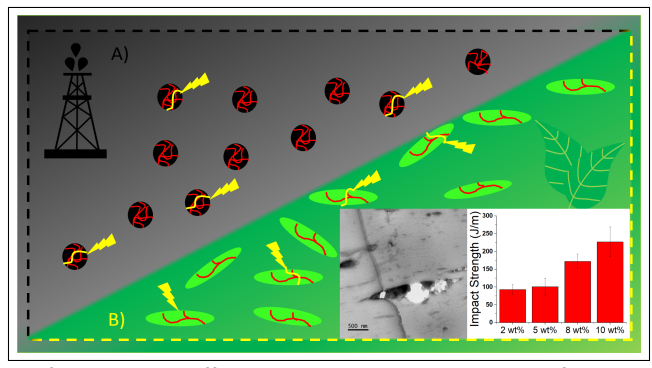
 Macromolecules 2019, -, DOI: 10.1021/acs.macromol.9b00707.
- (23) Lin, F.-Y.; Hohmann, A. D.; Hernández, N.; Shen, L.; Dietrich, H.; Cochran, E. W. Self-Assembly of Poly(styrene-block-acrylated epoxidized soybean oil) Star-Brush-Like Block Copolymers. <u>Macromolecules</u> 2020, <u>53</u>, 8095–8107, DOI: 10.1021/acs.macromol.0c00441, Publisher: American Chemical Society.
- (24) Yan, M.; Lin, F.-Y.; Cochran, E. W. Dynamics of Hyperbranched Polymers Derived from Acrylated Epoxidized Soybean Oil. Polymer 2017, 125, 117–125, DOI: 10.1016/j.polymer.2017.07.088.
- (25) Schubert, C.; Osterwinter, C.; Tonhauser, C.; Schömer, M.; Wilms, D.; Frey, H.; Friedrich, C. Can Hyperbranched Polymers Entangle? Effect of Hydrogen Bonding on Entanglement Transition and Thermorheological Properties of Hyperbranched Polyglycerol Melts. <u>Macromolecules</u> 2016, 49, 8722–8737, DOI: 10.1021/acs.macromol.6b00674, Publisher: American Chemical Society.

- (26) Valerio, O.; Pin, J. M.; Misra, M.; Mohanty, A. K. Synthesis of Glycerol-Based Biopolyesters as Toughness Enhancers for Polylactic Acid Bioplastic through Reactive Extrusion. ACS Omega **2016**, 1, 1284–1295, DOI: 10.1021/acsomega.6b00325.
- (27) Gramlich, W. M.; Robertson, M. L.; Hillmyer, M. A. Reactive Compatibilization of Poly(l-lactide) and Conjugated Soybean Oil. Macromolecules **2010**, 43, 2313–2321.
- (28) Mauck, S. C.; Wang, S.; Ding, W.; Rohde, B. J.; Fortune, C. K.; Yang, G.; Ahn, S.-K.; Robertson, M. L. Biorenewable Tough Blends of Polylactide and Acrylated Epoxidized Soybean Oil Compatibilized by a Polylactide Star Polymer. <u>Macromolecules</u> **2016**, <u>49</u>, 1605–1615.
- (29) Robertson, M. L.; Chang, K.; Gramlich, W. M.; Hillmyer, M. A. Toughening of Polylactide with Polymerized Soybean Oil. Macromolecules **2010**, 43, 1807–1814.
- (30) Yan, M.; Huang, Y.; Lu, M.; Lin, F.-Y.; Hernández, N. B.; Cochran, E. W. Gel Point Suppression in RAFT Polymerization of Pure Acrylic Cross-Linker Derived from Soybean Oil. <u>Biomacromolecules</u> 2016, <u>17</u>, 2701–2709, DOI: 10.1021/acs.biomac.6b00745.
- (31) Thompson, Z. J.; Hillmyer, M. A.; Liu, J. D.; Sue, H.-J.; Dettloff, M.; Bates, F. S. Block Copolymer Toughened Epoxy: Role of Cross-Link Density. Macromolecules 2009, 42, 2333–2335, DOI: 10.1021/ma900061b.
- (32) Wu, M.; Wang, K.; Zhang, Q.; Fu, Q. Manipulation of Multiphase Morphology in the Reactive Blending System OBC/PLA/EGMA. <u>RSC Advances</u> **2015**, <u>5</u>, 96353–96359, DOI: 10.1039/C5RA12271F, Publisher: The Royal Society of Chemistry.
- (33) Liu, W.; Qiu, J.; Zhu, L.; Fei, M.-e.; Qiu, R.; Sakai, E.; Ito, K.; Song, G.; Tang, G. Tannic Acid-Induced Crosslinking of Epoxidized Soybean Oil for Toughening Poly(lactic acid) via Dynamic Vulcanization. <u>Polymer</u> 2018, <u>148</u>, 109–118, DOI: 10.1016/j.polymer.2018.06.021.

- (34) Canetti, M.; Cacciamani, A.; Bertini, F. Miscible Blends of polylacand poly(methyl methacrylate): Structure, tide Morphology, and Ther-Behavior. Journal of Polymer Science Part B: Polymer Physics mal 2014. 1168-1177,52, DOI: https://doi.org/10.1002/polb.23544, eprint: https://onlinelibrary.wiley.com/doi/pdf/10.1002/polb.23544.
- (35) Xue, B.; He, H.; Zhu, Z.; Li, J.; Huang, Z.; Wang, G.; Chen, M.; Zhan, Z. A Facile Fabrication of High Toughness Poly(Lactic Acid) via Reactive Extrusion with Poly(Butylene Succinate) and Ethylene-Methyl Acrylate-Glycidyl Methacrylate. Polymers 2018, 10, 1401, DOI: 10.3390/polym10121401.
- (36) Ding, Y.; Feng, W.; Lu, B.; Wang, P.; Wang, G.; Ji, J. PLA-PEG-PLA Tri-Block Copolymers: Effective Compatibilizers for Promotion of the Interfacial Structure and Mechanical Properties of PLA/PBAT Blends. <u>Polymer</u> **2018**, <u>146</u>, 179–187, DOI: 10.1016/j.polymer.2018.05.037.
- (37) Mehrabi Mazidi, M.; Edalat, A.; Berahman, R.; Hosseini, F. S. Highly-Toughened Polylactide- (PLA-) Based Ternary Blends with Significantly Enhanced Glass Transition and Melt Strength: Tailoring the Interfacial Interactions, Phase Morphology, and Performance. Macromolecules 2018, 51, 4298–4314, DOI: 10.1021/acs.macromol.8b00557, Publisher: American Chemical Society.
- (38) Shang, M.; Wu, Y.; Shentu, B.; Weng, Z. Toughening of PBT by POE/POE- g GMA Elastomer through Regulating Interfacial Adhesion and Toughening Mechanism. <u>Industrial & Engineering Chemistry Research</u> **2019**, <u>58</u>, 12650–12663, DOI: 10.1021/acs.iecr.9b00691.
- (39) Chen, Y.; Wang, W.; Yuan, D.; Xu, C.; Cao, L.; Liang, X. Bio-Based PLA/NR-PMMA/NR Ternary Thermoplastic Vulcanizates with Balanced Stiffness and Toughness: "Soft-Hard" Core-Shell Continuous Rubber Phase, In Situ Compatibilization,

and Properties. ACS Sustainable Chemistry & Engineering 2018, 6, 6488-6496, DOI: 10.1021/acssuschemeng.8b00267, Publisher: American Chemical Society.

TOC Graphic



Schematic illustration comparing legacy petroleum-based entangled rubber impact modification with compostable bio-rubber toughening. A) Impact modifiers comprised of old carbon, long life cycle, petroleum-based, permanent elastomers with $G' \gg G''$. The spherical elastomeric cavities are depicted as dark circles containing highly entangled red rubbery chains. The lightning bolts represent propagating cracks, blunted by the elastomeric inclusions. B) Biobased, biodegradable, new carbon, circular life cycle rubbery hyper-branched polymers with $G' \ll G''$. Soybean derived elastomers dispersed in PLA are shown as green ellipsoidal inclusions composed of branched red chains. As with legacy elastomeric fillers, these soybean elastomer domains effectively arrest crack propagation through analogous cavitation mechanisms, dissipating mechanical energy as quantified through impact strength measurements.

Cavitation-Mediated Fracture Energy Dissipation in Polylactide at Rubbery Soybean Oil-based Block Copolymer Interfaces Formed via Reactive Extrusion

Baker W Kuehl, Austin Hohmann, Ting Han Lee, Michael Forrester, Nacu Hernandez, Hannah Dietrich, Connor Smith, Sam Musselman, Grayson Tran, and Eric W. Cochran*

Department of Chemical & Biological Engineering, Iowa State University, Ames, Iowa 50011, United States

E-mail: ecochran@iastate.edu

Supplementary Information

List of Figures

S1	Example of Polymerization Route to produce SBCP series polymers	S-7
S2	Time-temperature superposition (TTS) of the terminal region of PAEHOSO	
	homopolymer at a reference temperature of $20^{\circ}\mathrm{C}$	S-7
S3	DSC traces for the SBCP series polymer blends	S-8
S4	GPC traces for the the precursor block for the SBCP polymers	S-8
S5	Examples of the various polymer architectures blended into the PLA matrix	S-8

S6	Viscosity measurements of PMAEHOSO vs PAEHOSO at 80°C	S-9
S7	Tg's of the varying pure homopolymers and statistical copolymers used in the	
	PLA blends	S-9
S8	The Following SEM micrographs show the IZOD impact surface of the SBCP	
	polymer blend series. A) SBCP-A Low MAG, B) SBCP-B Low MAG, C)	
	SBCP-C Low MAG, D) SBCP-D Low MAG, E) SBCP-A High MAG, F)	
	SBCP-B High MAG, G) SBCP-C High MAG, H) SBCP-D High MAG. The	
	circles indicate areas for rubber particle cavitation behavior	S-10
S9	Stress vs Strain Curves for SBCP-B-blends at varying Loadings	S-10
S10	Impact Strength Values for SBCP-B-blends at varying Loadings	S-11
S11	Chemical structure and proton assignments for AEHOSO	S-11

Experimental Methods

Materials

Epoxidized High Oleic Soybean Oil (EHOSO) was kindly supplied by CHS, triethylamine (TEA), hydroquinone (HQ), and acrylic acid (AA) were all purchased from Sigma Aldrich with purity of 99% or higher. Carbon Disulfide (CS₂), ethane thiol (C₂H₆S), p-tosyl chloride and azobisisobutyronitrile (AIBN) were purchased from Sigma Aldrich. Glycidyl methacrylate (GMA), 2,2'-azodi(2-methylbutyronitrile) (AMBN), and dioxane were purchased from Sigma Aldrich with purities of 98% or higher. Methanol was purchased from Fischer scientific with a purity of 99.8%.

Acrylation of Epoxidized High Oleic Soybean Oil (AEHOSO)

100g of EHOSO (0.103 mol), 27.5g of AA (0.319 mol), 0.893g TEA (0.7% w/w of EHOSO) and 1.6g HQ (1.25% w/w of EHOSO) were added in a round bottom. The reaction was allowed to react 4 h at 110 $^{\circ}$ C in a round bottom flask equipped with rubber septa to achieve

an acrylic functionality 2.15 eq AA/eq EHOSO. After the reaction is done, distillation was performed at 100 degrees °C under vacuum in order to remove excess AA. ¹H-NMR (Bruker, AVIII, 600 MHz) in deuterated chloroform (CDCl₃) was used to confirm structure and purity (assignments refer to Figure S11): δ 0.8–1.1 ppm (t, 9H, H_a, δ 2.2–2.4 ppm (m, 6H, H_b), δ 4.2–4.4 ppm (m, 4H, H_c), δ 5.3 ppm (s, H, H_d), δ 5.70–6.5 ppm (m, 3H, H_{e,f})

RAFT Polymerization of Acrylated Epoxidized High Oleic Soybean oil

50g of AEHOSO (.0454 mol), 0.1894g of 2,2-Azobis(2-methylpropionitrile) (0.00115 mol), 0.0157g (77 μ mol) of 2-Ethyl (3-oxobutan-2-yl) carbonotrithioate (OxCART), and 51.5g of dioxane were added to a round bottom flask equipped with a stirbar. The reaction vessel was purged for 30 minutes with argon and proceeded with the reaction at 80 degrees C for 2 hours. The reaction was quenched by the addition of hydroquinone at 0.1% by wt of the reaction contents. A small sample of the reaction was precipitated in menthol and n-hexanes for analysis with GPC and 1H-NMR. 1H-NMR (Bruker, AVII, 600 MHz) in CDCl₃ was used to confirm structure and purity (assignments refer to Figure S11): δ 0.8–1.1 ppm (t, 9H, H_a), δ 2.2–2.4 ppm (m, 6H, H_b), δ 4.2–4.4 ppm (m, 4H, H_c), δ 5.3 ppm (s, H, H_d), δ 5.70–6.5 ppm (m, 3H, H_{e,f})

RAFT Polymerization of Methacrylated Epoxidized High Oleic Soybean oil stat- Poly Methyl Methacrylate

50g of Acrylated Epoxidized High Oleic Soybean Oil (41.8 mmol), 22g of methyl methacrylate (0.2195 mol), 0.01383g of 2,2-Azobis(2-methylpropionitrile) (0.11 mmol), 0.02951g (0.24 mmol) of 2-cyanopropan-2-yl methyl carbonotrithioate (CYCART), and 72g of dioxane were added to a round bottom flask equipped with a stirbar. The reaction vessel was purged for 30 minutes with argon and proceeded with the reaction at 80 °C for 2 h. The reaction was

quenched by the addition of hydroquinone at 0.1% by wt of the reaction contents. A small sample of the reaction was precipitated in menthol and n-hexanes for analysis with GPC and ¹H-NMR. ¹H-NMR (Bruker, AVII, 600 MHz) in CDCl₃ was used to confirm structure

RAFT Polymerization of Glycidyl Methacrylate (PGMA-CTA)

30g of glycidyl methacryalate (0.2113 mol), 0.1153g of 2,2-Azobis(2-methylpropionitrile) (6 mmol), 0.615g (3 mmol) of 2-cyanopropan-2-yl methyl carbonotrithioate (CYCART), and 31g (0.3517 mol) of Dioxane were added to a round bottom flask equipped with a stirbar. The reaction vessel was purged for 30 minutes with argon and proceeded with the reaction at 80 °C for 4 hours. The reaction was precipitated in methanol and dried at 50 °C overnight. A small sample was then taken to perform gel permeation chromatography (GPC) to determine molecular weight.

RAFT Polymerization of Glycidyl Methacrylate-b-Poly Acrylated Epoxidized High Oleic Soybean Oil

12g (10 mmol) of AEHOSO, 3g (0.062236 mol) of PGMA-RAFT CTA, 0.05768g (0.00119 mol) of AMBN, and 33.14g (0.376 mol) of dioxane were added to a round bottom flask equipped with a stirbar. The reaction vessel was purged for 30 minutes and then the reaction proceeded at 80 °C for 2.5 h. The reaction was then precipitated in methanol and dried. A small sample was taken for NMR to determine composition. ¹H-NMR (Bruker, AVII, 600 MHz) in CDCl₃ was used to confirm the structure and composition.

Preparation of Polymer Blends

The fabrication of the A+B polymer blends were performed by first solvent blending a calculated amount of polymer modifier with various amounts of PLA in 350g of chloroform depending on the composition. The mixture was then dried at 60 °C for 2 d prior to melt

blending. The polymer was then melt blended using a Haake miniLab twin screw extruder. The extrudate was cooled and prepared for injection molding. The blends were synthesized at $220~^{\circ}$ C with a 10~minute residence time at 65~RPM.

Preparation of Mechanical Property Test Specimens

The extrudate was used to make ASTM D256 IZOD bars and ASTM D638 Type 5 dogbones. A Haake MiniJet injection molder was used with the barrel temperature set to 240 °C and a mold temperature of 40 °C. The Ram pressure was set to 700 bar. Notches were then created under the ASTM D256 Specifications.

Mechanical Property Tests

Uniaxial tensile tests were performed with an Instron 3367 Tensile Tester using a cross-head moving rate of 5mm/min. Impact Tests were conducted using a Tinius Olsen 527. The value reported was represented as an average over 5 specimens.

Analysis of Microstructure

Analysis of microstructure was performed on a 200kV JEOL 2100 Scanning/Transmission Electron Microscope. Each TEM specimen was ultra-microtomed at -70 °C in the whitened gauge region of the tensile bar. SEM was performed on the IZOD fracture surfaces using a FEI Quanta 250 FE-SEM.

Rheology

Rheology was run on an Ares G2 rheometery using 8mm parallel plate geometry. The master curve was generated by varying the frequency from 100 rad/s to .1 rad/s. The temperature range was from 30 °C to -10 °C with 10 °C increments. Viscosity measurements were also performed with an 8mm parallel plate geometry with shear rates from .1-1 Hz

Dynamic Scanning Calorimetry

Modulated DSC was performed using a Discover 2500. The samples were dried at 100°C prior to undergoing a 2°C/min ramp from -100°C to 150°C

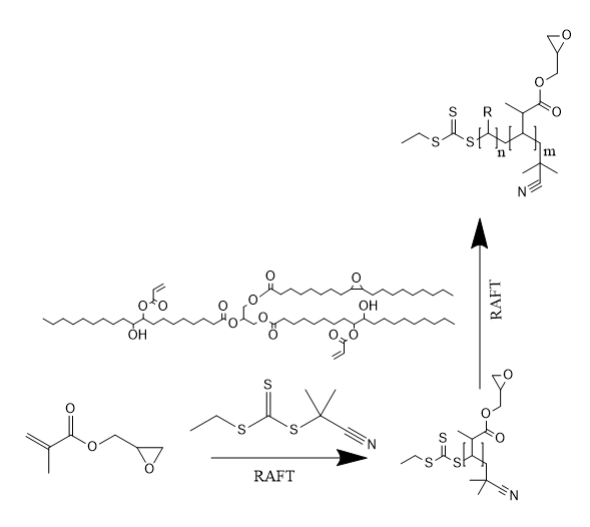


Figure S1: Example of Polymerization Route to produce SBCP series polymers

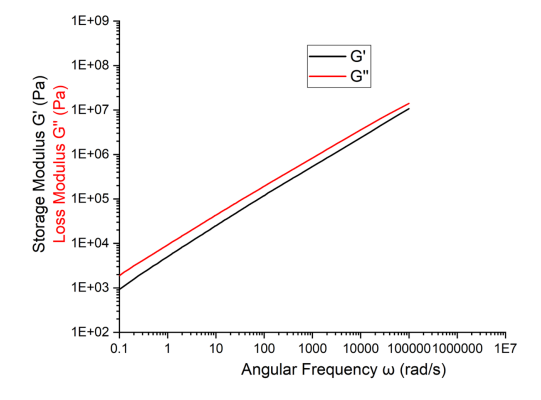


Figure S2: Time-temperature superposition (TTS) of the terminal region of PAEHOSO homopolymer at a reference temperature of $20^{\circ}\mathrm{C}$

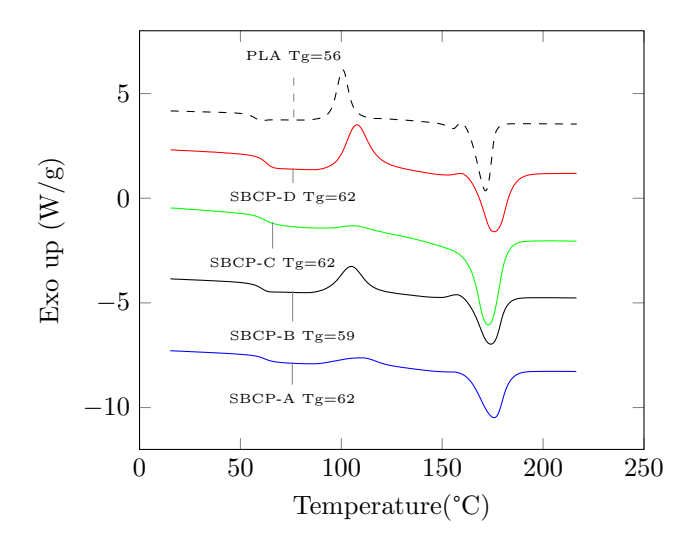


Figure S3: DSC traces for the SBCP series polymer blends

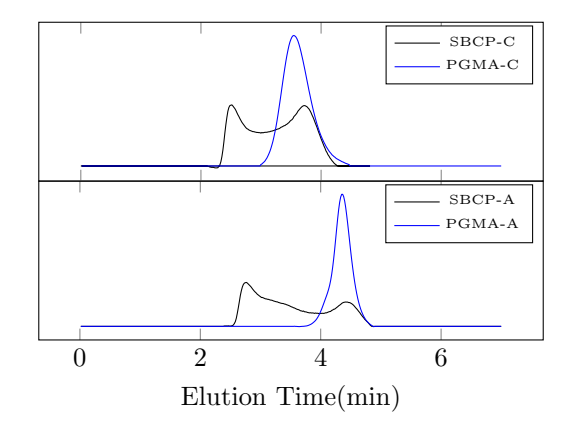


Figure S4: GPC traces for the the precursor block for the SBCP polymers

Figure S5: Examples of the various polymer architectures blended into the PLA matrix

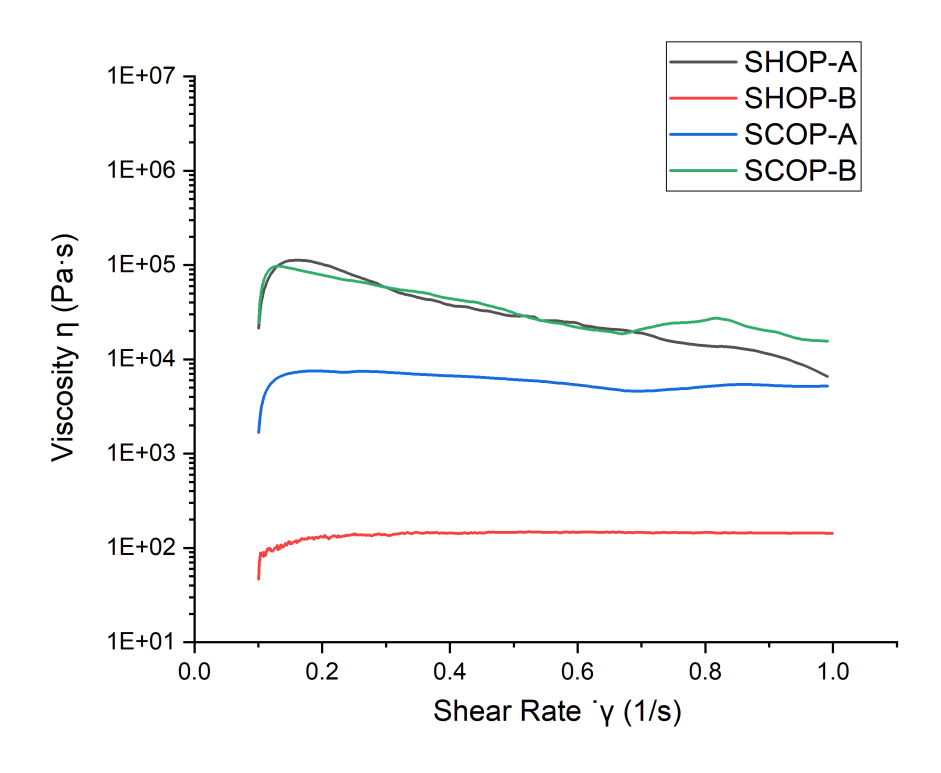


Figure S6: Viscosity measurements of PMAEHOSO vs PAEHOSO at 80°C

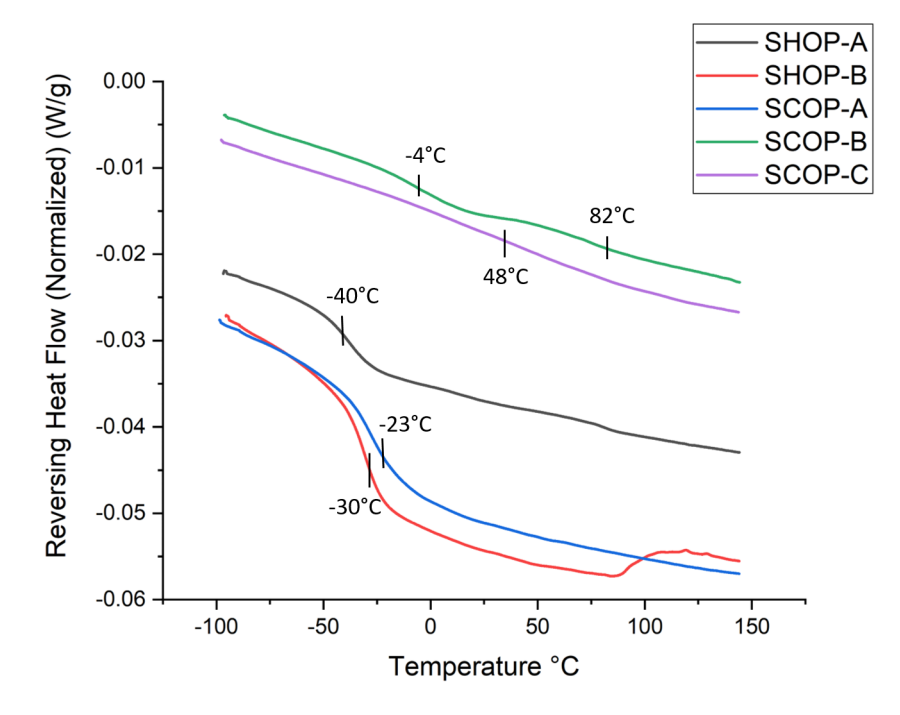


Figure S7: Tg's of the varying pure homopolymers and statistical copolymers used in the PLA blends

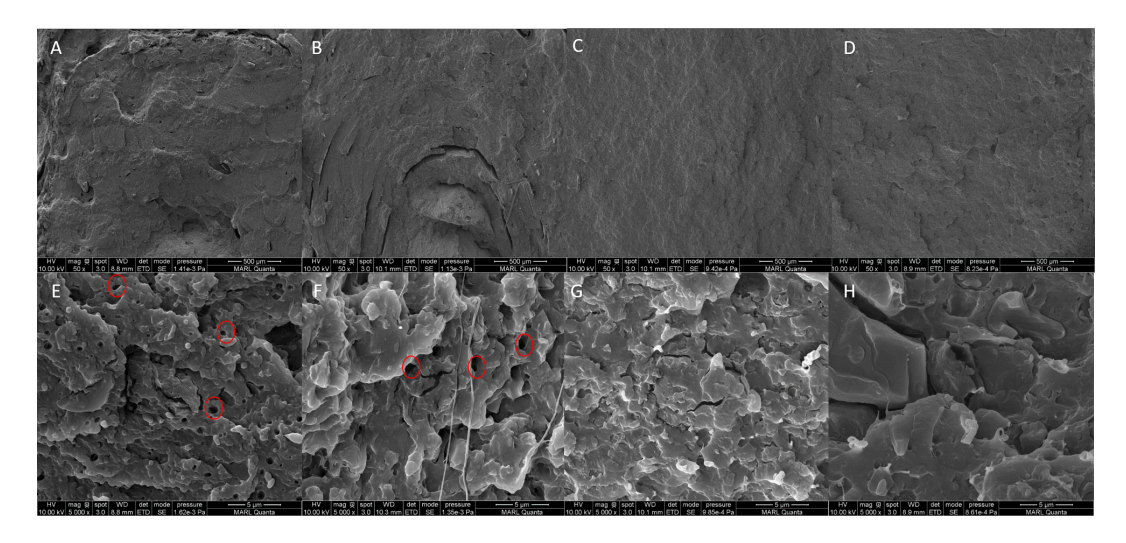


Figure S8: The Following SEM micrographs show the IZOD impact surface of the SBCP polymer blend series. A) SBCP-A Low MAG, B) SBCP-B Low MAG, C) SBCP-C Low MAG, D) SBCP-D Low MAG, E) SBCP-A High MAG, F) SBCP-B High MAG, G) SBCP-C High MAG, H) SBCP-D High MAG. The circles indicate areas for rubber particle cavitation behavior.

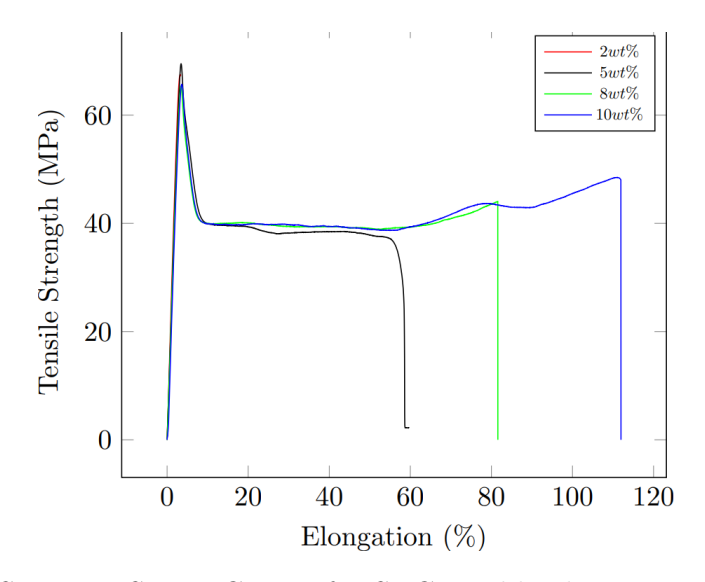


Figure S9: Stress vs Strain Curves for SBCP-B-blends at varying Loadings

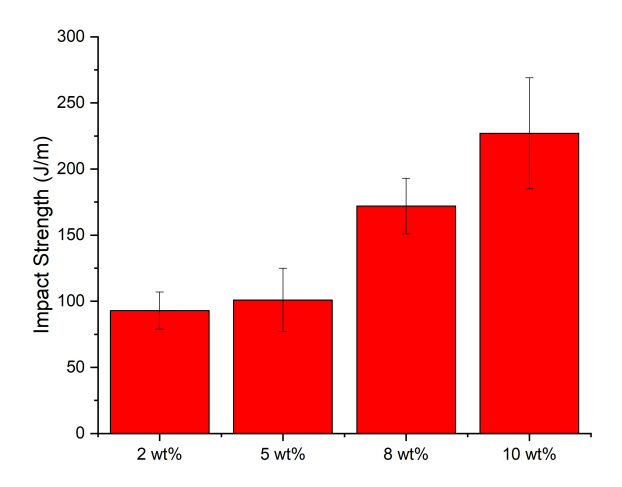


Figure S10: Impact Strength Values for SBCP-B-blends at varying Loadings

Figure S11: Chemical structure and proton assignments for AEHOSO.